

Dark Regions of No-Reflow on Late Gadolinium Enhancement Magnetic Resonance Imaging Result in Scar Formation After Atrial Fibrillation Ablation

Christopher McGann, MD, Eugene Kholmovski, PhD, Joshua Blauer, BS, Sathya Vijayakumar, MS, Thomas Haslam, BS, Joshua Cates, PhD, Edward DiBella, PhD, Nathan Burgon, BS, Brent Wilson, MD, PhD, Alton Alexander, BS, Marcel Prastawa, PhD, Marcos Daccarett, MD, Gaston Vergara, MD, Nazem Akoum, MD, Dennis Parker, PhD, Rob MacLeod, PhD, Nassir Marrouche, MD
Salt Lake City, Utah

- Objectives** The aim of this study was to assess acute ablation injuries seen on late gadolinium enhancement (LGE) magnetic resonance imaging (MRI) immediately post-ablation (IPA) and the association with permanent scar 3 months post-ablation (3moPA).
- Background** Success rates for atrial fibrillation catheter ablation vary significantly, in part because of limited information about the location, extent, and permanence of ablation injury at the time of procedure. Although the amount of scar on LGE MRI months after ablation correlates with procedure outcomes, early imaging predictors of scar remain elusive.
- Methods** Thirty-seven patients presenting for atrial fibrillation ablation underwent high-resolution MRI with a 3-dimensional LGE sequence before ablation, IPA, and 3moPA using a 3-T scanner. The acute left atrial wall injuries on IPA scans were categorized as hyperenhancing (HE) or nonenhancing (NE) and compared with scar 3moPA.
- Results** Heterogeneous injuries with HE and NE regions were identified in all patients. Dark NE regions in the left atrial wall on LGE MRI demonstrate findings similar to the “no-reflow” phenomenon. Although the left atrial wall showed similar amounts of HE, NE, and normal tissue IPA ($37.7 \pm 13\%$, $34.3 \pm 14\%$, and $28.0 \pm 11\%$, respectively; $p = \text{NS}$), registration of IPA injuries with 3moPA scarring demonstrated that $59.0 \pm 19\%$ of scar resulted from NE tissue, $30.6 \pm 15\%$ from HE tissue, and $10.4 \pm 5\%$ from tissue identified as normal. Paired *t*-test comparisons were all statistically significant among NE, HE, and normal tissue types ($p < 0.001$). Arrhythmia recurrence at 1-year follow-up correlated with the degree of wall enhancement 3moPA ($p = 0.02$).
- Conclusions** Radiofrequency ablation results in heterogeneous injury on LGE MRI with both HE and NE wall lesions. The NE lesions demonstrate no-reflow characteristics and reveal a better predictor of final scar at 3 months. Scar correlates with procedure outcomes, further highlighting the importance of early scar prediction. (J Am Coll Cardiol 2011;58:177–85) © 2011 by the American College of Cardiology Foundation

Atrial fibrillation (AF) is the most common cardiac rhythm disturbance affecting more than 2 million people in the

United States (1,2). Pulmonary vein isolation using radiofrequency ablation (RFA) is effective in symptomatic, drug-refractory AF and can result in cure. With current technology, the procedure is guided using x-ray fluoroscopy, with tissue viability and lesion localization provided by electro-anatomical mapping (EAM) systems. Catheter navigation has been enhanced by use of 3-dimensional (3D) left atrial (LA) angiograms acquired with magnetic resonance imaging (MRI) or computed tomography. Despite these advancements in technology, reported success rates of the procedure vary significantly with AF recurrence ranging from 25% to 60% (3–6). The high failure rate is in part

From the Comprehensive Arrhythmia Research and Management Center, University of Utah, Salt Lake City, Utah. This study was funded by a Seed Grant from the University of Utah. This work was made possible in part by software from the National Center for Research Resources Center for Integrative Biomedical Computing (P41-RR12553-10 and 2P41 RR0112553-12) and the National Alliance for Medical Image Computing, funded by the National Institutes of Health (NIH) through the NIH Roadmap for Medical Research, grant U54 EB005149. Drs. Marrouche, Parker, DiBella, and Kholmovski receive support from SurgiVision. All other authors have reported that they have no relationships to disclose.

Manuscript received January 4, 2011; revised manuscript received March 18, 2011, accepted April 19, 2011.

**Abbreviations
and Acronyms****3D** = 3-dimensional**3moPA** = 3 months
post-ablation**AF** = atrial fibrillation**HE** = hyperenhancing**IPA** = immediately
post-ablation**LA** = left atrial**LGE** = late gadolinium
enhancement**MRI** = magnetic resonance
imaging**NE** = nonenhancing**RF** = radiofrequency**RFA** = radiofrequency
ablation

attributable to the limited information on the location, extent, and permanence of LA wall injury during and after ablation, which has proven difficult to assess with EAM alone.

More recently, powerful tools to better assess RFA lesions have been developed with MRI. Visualization and characterization of RFA lesions were demonstrated by Lardo *et al.* (7) in a canine model with T2-weighted and contrast-enhanced T1-weighted imaging. Late gadolinium enhancement (LGE) and T2-weighted (T2w) double inversion recovery (DIR) sequences are now used in humans to evaluate periprocedural injuries, and these

imaging advances have helped define the early and late tissue events and the atrial remodeling process after ablation. Transient injury has been demonstrated on T2w DIR imaging and reflects edema and the inflammatory process (8–10). Permanent injury with LA wall scarring has been well studied using LGE in the weeks to months after the procedure. The location and degree of scarred tissue appears bright on LGE MRI and has been associated with procedure outcomes. Furthermore, LGE can help guide follow-up ablations by identifying gaps in ablation lines after unsuccessful pulmonary vein isolation (11–14).

Though these imaging advances have helped define post-ablation injuries, early imaging markers to predict permanent injury remain elusive. In this study, we set out to characterize early atrial wall injury immediately post-ablation (IPA) using LGE MRI and its potential to predict permanent scar 3 months post-ablation (3moPA).

Methods

Patients. From July 2009 to January 2010, 46 patients who underwent first ablation for AF in our electrophysiology-MRI suite were included in the study. This group was selected on the basis of patients who completed MRI scans at baseline, IPA, and 3moPA. Further selection criteria included LGE images acquired 15 ± 3 min after contrast injection in the IPA and 3moPA scans. The protocol was approved by the institutional review board at the University of Utah and was compliant with the Health Insurance Portability and Accountability Act of 1996. Scanning was performed using a 3-T Verio MR scanner (Siemens Medical Systems, Erlangen, Germany). MRI for IPA scans was performed <1 h after completion of the RFA procedure.

MRI acquisitions. High-resolution LGE images of the left atrium were acquired 15 ± 3 min after the injection of 0.1 mmol/kg gadolinium contrast (Multihance, Bracco

Diagnostics, Inc., Princeton, New Jersey) using a 3D respiratory navigated, inversion recovery prepared gradient echo pulse sequence (repetition time 3.0; echo time 1.4 ms; flip angle 14° ; bandwidth 740 Hz/pixel; field of view $400 \times 400 \times 110$ mm; matrix size $320 \times 320 \times 44$; 9% oversampling in the slice encoding direction; voxel size $1.25 \times 1.25 \times 2.5$ mm; phase-encoding direction: left to right; fractional readout 87.5%; partial Fourier acquisition: 90% in phase-encoding direction and 92.5% in slice-encoding direction; generalized autocalibrating partially parallel acquisitions with $R = 2$ in phase-encoding direction). An inversion pulse was applied every heartbeat, and fat saturation was applied immediately before data acquisition. Data acquisition was limited to 15% of the RR cycle and was performed during LA diastole. To preserve magnetization preparation in the image volume, the navigator was acquired immediately after data acquisition block. Typical scan time for the LGE study was 4 to 8 min, depending on heart rate and respiratory pattern.

Ablation procedure. The details of the pulmonary vein isolation in addition to posterior wall and septal debulking have been described elsewhere (13). Briefly, the left atrium was accessed through 2 transseptal punctures under intracardiac echocardiographic guidance using a phased-array catheter (Acunav, Siemens Medical Solutions USA, Inc., Mountain View, California). A 10-pole circular mapping catheter (Lasso, Biosense Webster, Diamond Bar, California) and a 3.5-mm Thermocool ablation catheter (Biosense Webster) were advanced into the left atrium for mapping and ablation. A 14-pole catheter (TZ Medical, Portland, Oregon) was used to record right atrial and coronary sinus electrograms and was used as the reference catheter for 3D electroanatomical mapping with CARTO (Biosense Webster). Radiofrequency (RF) energy was delivered with 50 W at a catheter tip temperature of 50°C for 5 s, guided by electrogram abolition recorded on the Lasso catheter. Ablation lesions were placed in a circular fashion in the pulmonary vein antral region until electrical isolation of the pulmonary veins was achieved. Additional lesions were placed along the LA posterior wall and septum.

Image processing and analysis. All magnetic resonance images were evaluated and processed by 2 expert operators using Seg3D image analysis software. The LA wall in the 3D LGE MRI acquisitions was manually segmented with careful tracing of the endocardial and epicardial borders. Tissue types were determined using a threshold-based lesion detection algorithm previously described (9,15). Briefly, tracings were performed to confine the region of interest to the LA wall alone and to avoid the blood pool. Normal, nonenhanced (NE), and hyperenhanced (HE) tissue was defined on the basis of 3 distinct modes of LA wall tissue intensities. Each patient scan was evaluated independently, with the mean normal LA wall segments first defined for each patient. HE and NE tissue injury was defined at 3 standard deviations above and below the normal tissue mean pixel intensity, respectively. Tissue characterizations were

verified independently to ensure appropriate categorization. In the IPA images, we classified tissue as NE, HE, or normal. In the 3moPA images, tissue was classified as either normal or scar. The area per slice for each LA tissue type (normal, acute HE and NE, and 3-month scar) was summed for the entire scan and reported as a ratio of tissue volume to total LA wall volume.

To analyze the relationship between tissue types in IPA and 3moPA images, we performed a point-by-point quantitative analysis of the changes between tissue types in the wall regions of 10 LGE MRI patient scans. Scans for study were chosen as those images exhibiting the best quality as determined subjectively by the 2 operators and analyzed according to the following procedure. Using the LA wall segmentation and tissue typing data previously obtained, we classified each tissue voxel according to type. Next, we generated 3D surface mesh models for all endocardial contours and projected the tissue classifications onto those surfaces using SCIRun data processing and visualization software. Finally, to compare tissue classifications at matching locations on IPA and 3moPA surfaces, we used mappings generated through the nonlinear, deformable surface registration method proposed by Glaunes and colleagues (16,17) following the computation scheme described by Ha et al. (18). This registration method does not require correspondence between the surface points and thus can be used to map surfaces that are composed of different numbers of points without manual definition of landmark points. In the application of the surface-matching technique derived from that of Glaunes and colleagues, the mean shift of surface points from before to after deformation was 5.2 ± 2.8 mm. This demonstrates that the extent of deformation necessary to match 1 surface to another is relatively small. To further demonstrate the ability of the algorithm to restore a surface to its original condition after an unknown deformation, a known nonrigid deformation was applied to the IPA surface. This known deformation induced a mean shift in node location of 3.0 ± 1.6 mm. The surface-matching algorithm was then applied to restore the deformed surface to its original form. After registration, the mean distance between each node and its original location was 1.0 ± 0.5 mm. The error introduced from these registration methods is relatively small and appears suitable for the LA wall structure. After model registration, the regions defined as scar on the 3moPA surface were mapped onto the IPA surface by matching locations to the 3 tissue classifications (NE, HE, and normal tissues).

Statistical analysis. Quantified scar is reported as a continuous variable as mean \pm SD. Proportions representing NE, HE, and normal tissue were compared using 3 paired Student *t* tests. Group means were considered significantly different if a *p* value <0.05 was obtained. Interobserver variability was calculated using Pearson's correlation coefficient. Statistical analysis was performed using SPSS version 15.0 (SPSS, Inc., Chicago, Illinois) and Stata version 11 (StataCorp LP, College Station, Texas).

Results

Patient data. Forty-six patients who underwent first ablation treatment for AF and completed the MRI scanning protocol at all 3 time points (baseline, IPA, and 3moPA) were eligible for inclusion in the study. The baseline scans were used to confirm normal pre-ablation LA wall and before including subjects for post-ablation analysis. Eight of the 46 patients were excluded because of inadequate LGE magnetic resonance images, 5 resulting from patient motion and 3 due to gating problems. An additional 1 patient was excluded after the discovery of a previous LA ablation procedure when LA wall hyperenhancement was seen on the baseline scan. Data from the remaining 37 patients were included in the study.

Each 3D LGE MRI scan resulted in approximately 20 to 30 axial slices to cover the entire left atrium depending on the size and shape of the chamber. For the 37-patient cohort, we segmented a total of 1,852 slices from the IPA and 3moPA scans (37 patients \times 2 scans \times 20 to 30 slices per patient). Two hundred sixty-two slices from the extreme superior and inferior surfaces of the left atrium were excluded from the computational analyses because of partial volume effects with minimal amount of LA tissue. Results from the remaining 1,590 slices, approximately one-half from each scan time point, were included in the quantitative data.

Lesion imaging on LGE MRI. In each subject (37 of 37 [100%]) who underwent RFA for AF, acute tissue injury IPA was seen as heterogeneous on LGE MRI. Ablated tissue demonstrated regions of differing contrast with bright HE as well as dark NE regions (Fig. 1). These imaging findings were seen <1 h after the completion of AF ablation, when the LGE sequence is performed approximately 15 min after contrast injection. When comparing early and late LGE imaging, we routinely found that regions of NE tissue IPA become enhanced 3moPA, suggesting that NE tissue represents ablation injury that results in necrosis and eventual scar (Fig. 2).

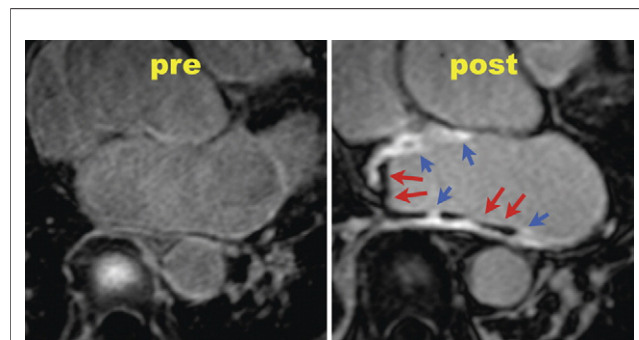


Figure 1 Heterogeneous LA Wall Injury

Typical left atrial (LA) wall characteristics on late gadolinium enhancement <1 h after radiofrequency ablation (right) with corresponding pre-ablation images (left). Injured left atrium shows both hyperenhancing (blue arrows) and non-enhancing (red arrows) tissue.

Acute LGE injury and association with permanent scar. Quantification of the degree of LA wall injury IPA and 3moPA showed a significantly greater amount of tissue injury on the IPA scans. We analyzed data from 1,590 segmented slices from IPA and 3moPA scans, approximately one-half from each, and found similar amounts of HE, NE, and normal tissue ($37.7 \pm 13\%$, $34.3 \pm 14\%$, and $28.0 \pm 11\%$, respectively; $p = 0.87$, 0.64 , and 0.76 using 3 paired t -test comparisons) (Fig. 3). A reasonable measure of the total extent of IPA injury was obtained by combining the NE and HE tissue volumes, which summed to 72.0% of the LA wall. However, the extent of permanent LA wall injury 3moPA was much smaller, with scarring in $33.9 \pm 8\%$ of the LA wall (Fig. 4). These data demonstrate poor correlation of the combined acute injuries with scar at 3 months.

We next investigated the degree of scarring that resulted from either NE or HE tissue. To do this, we performed a detailed quantitative analysis of the LGE MRI injuries seen IPA and 3moPA using 3D nonrigid deformation processing

methods described earlier. These processing methods were labor intensive and thus were performed on a subset of 10 patients with the best image quality MRI scans. A total of 498 segmented slices from IPA and 3moPA scans (approximately one-half from each) were included in the 3D analysis. Using these methods, we found that $59.0 \pm 19\%$ of scar resulted from NE tissue, $30.6 \pm 15\%$ from HE tissue, and $10.4 \pm 5\%$ from tissue identified as normal. Paired t -test comparisons were all statistically significant, including NE versus HE ($p = 0.0016$), NE versus normal ($p < 0.0001$), and HE versus normal ($p = 0.0008$) (Figs. 5 and 6). Nearly 2-fold more scarring resulted from NE compared with HE injury (59.0% vs. 30.6%). These data reveal significant differences in the relative contribution of acute NE and HE injury to scar at 3 months.

Tissue injury with “no-reflow” characteristics. Dark NE regions in the LA wall after ablation demonstrate findings compatible with the no-reflow phenomenon. These findings are best demonstrated on LGE when imaging is performed at different time intervals after the administration

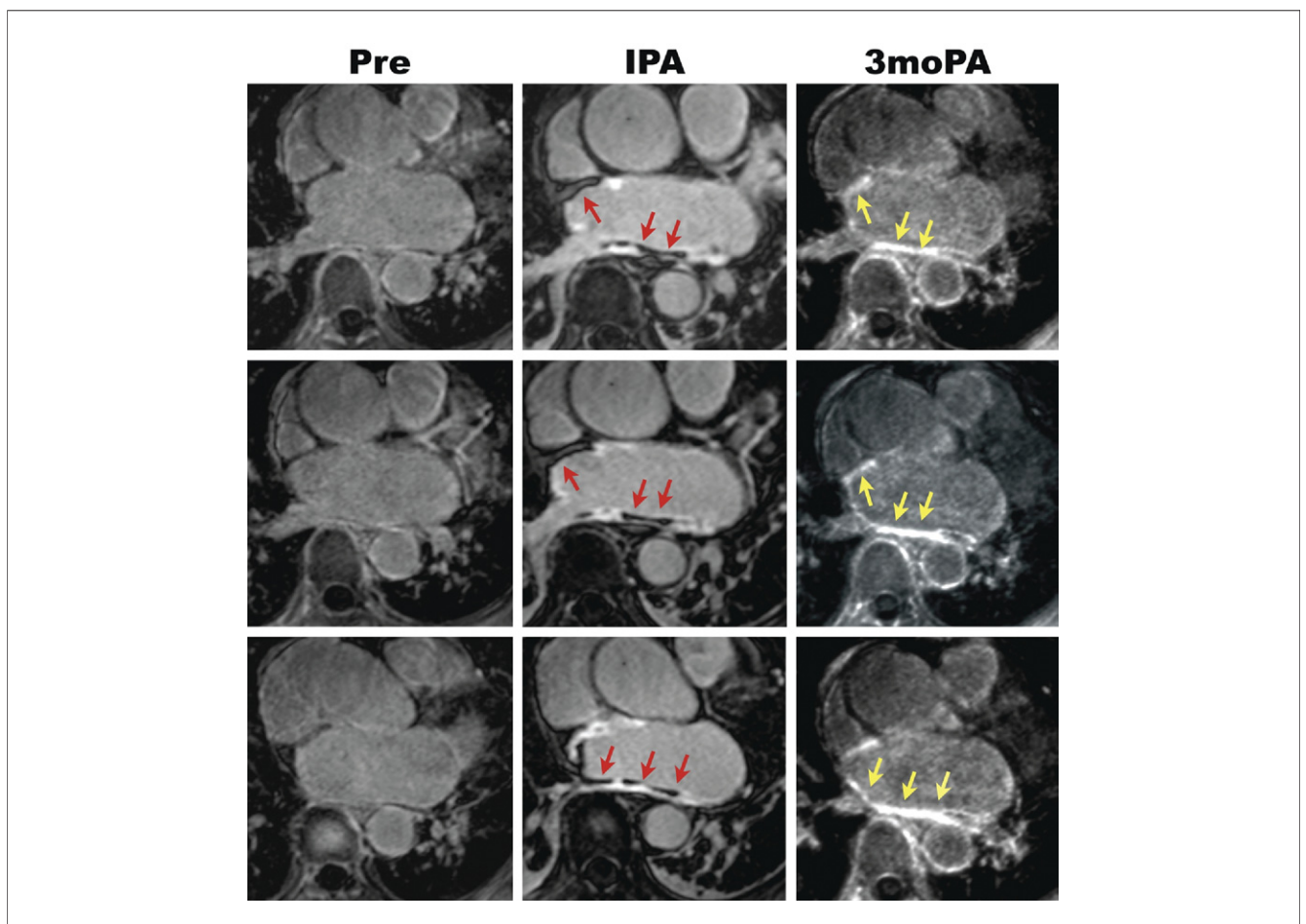


Figure 2 Acute Left Atrial Wall Injury and Scar Remodeling

Immediate post-ablation (IPA) injury (middle) shows extensive damage with nonenhancing (NE) and hyperenhancing lesions on late gadolinium enhancement (LGE). Dark NE regions of no-reflow (red arrows) later enhance 3 months post-ablation (3moPA) and predict scar (yellow arrows). Serial LGE imaging studies are shown with closely matched slices: pre-ablation (left), IPA (middle), and 3moPA (right).

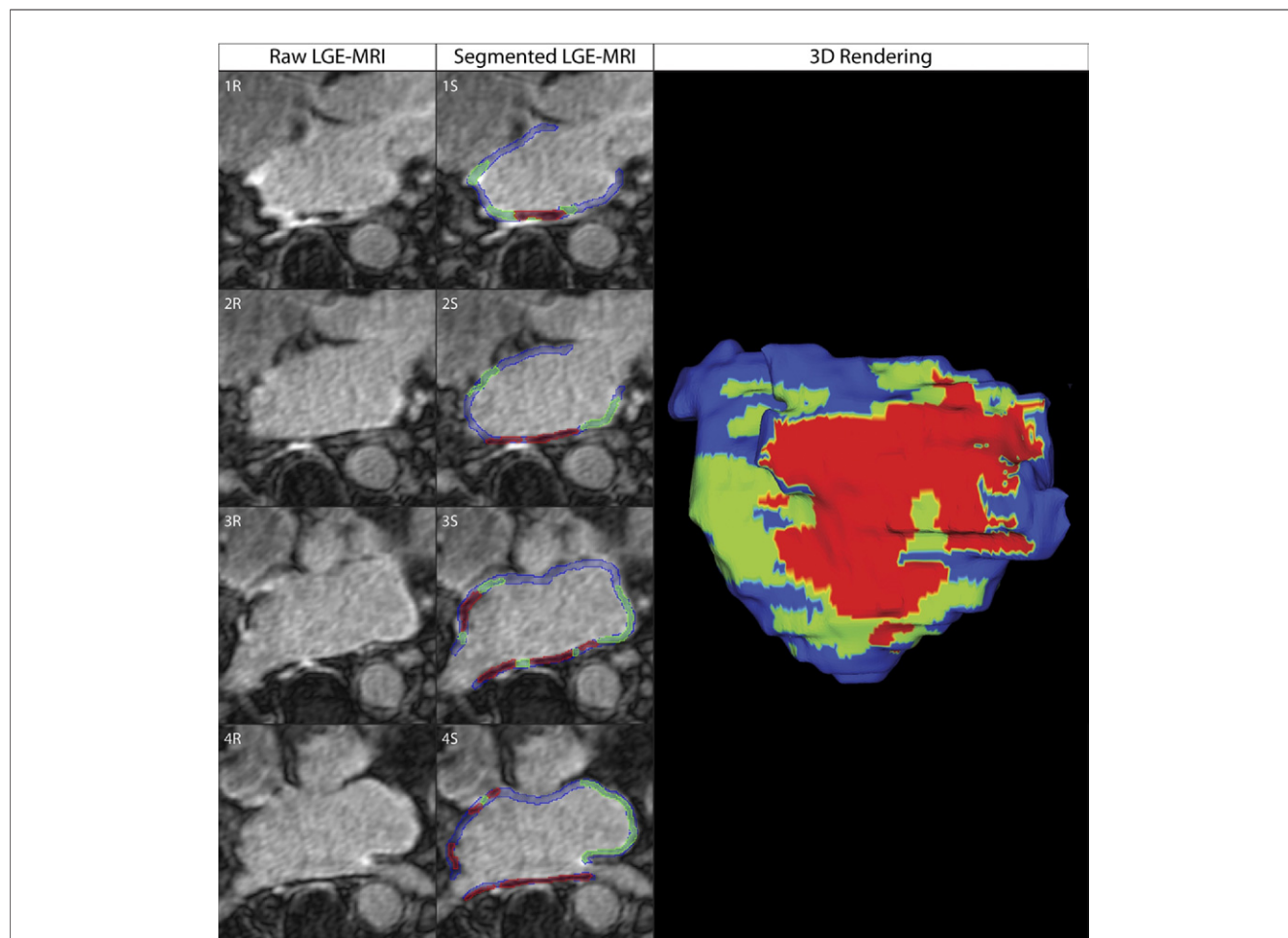


Figure 3 Segmentation Process Used for Quantification of Left Atrial Wall Injury on IPA Scans

Injuries were determined using set thresholds above and below the defined normal wall regions. Normal uninjured tissue is shown in **blue**, nonenhancing tissue in **red**, and hyperenhancing tissue in **green**. LGE = late gadolinium enhancement; MRI = magnetic resonance imaging; 3D = 3-dimensional.

of gadolinium contrast (Fig. 7). On standard LGE imaging 15 min after contrast injection, we identified large regions of NE tissue within the LA wall along with HE regions (Figs. 7A1 and 7A2). When LGE imaging was performed at a longer time interval after the administration of gadolinium contrast, we saw progressive enhancement of the tissue initially seen as NE (Figs. 7B1 and 7B2).

Interobserver reproducibility. Two operators performed wall tracings, and a high degree of interobserver correlation for the LA endocardial and epicardial wall tracings was observed for both the IPA ($r = 0.98$; 95% confidence interval: 0.94 to 0.99; $p < 0.001$) and 3moPA ($r = 0.99$; 95% confidence interval: 0.94 to 0.99; $p < 0.001$) scans. The high degree of correlation reflects the good scan quality as well as the experience of the operators in our laboratory, who perform these tracings on a regular basis with the aid of computer processing tools in SCIRun.

LA wall scarring at 3 months and patient outcomes. One year post-ablation, 29 of 37 patients (78.4%) remained free of AF. When dividing patients into quartiles on the basis of

percentage of LA wall scar on LGE 3moPA, a significant difference was seen between responders and nonresponders (Fig. 8). Patients in the fourth quartile, defined as moderate scar formation (LA wall scar $>23\%$) had no AF recurrence at 1-year follow-up. In comparison, all 8 recurrences occurred in patients in the lower quartiles with mild scar formation (LA wall scar $\leq 23\%$) ($p = 0.02$). Because there were no recurrences in the first quartile, an odds ratio could not be calculated.

Discussion

Main findings. In this study, we describe acute injuries caused by RF ablation with NE and HE tissue types on LGE MRI. While ablation injury is known to hyperenhance on LGE, NE regions consistent with no-reflow have not been described previously in the LA myocardium and appear to predict permanent scar.

Acute LA wall injuries on LGE MRI. In patients with AF undergoing their first ablation procedure, extensive

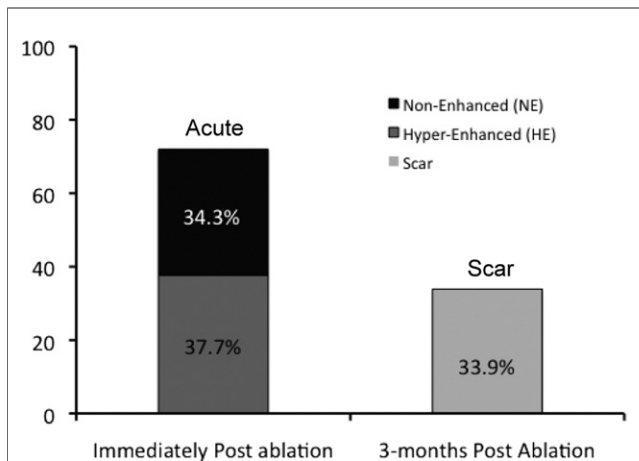


Figure 4 Comparison of Acute Injuries Immediately Post-Ablation to Scar 3 Months Post-Ablation

The early global injury on late gadolinium enhancement (nonenhanced [NE] + hyperenhanced [HE] = 72.0%) does not correlate well with late scar (33.9%). HE $37.7 \pm 12\%$, NE $34.3 \pm 13\%$, scar $33.9 \pm 8\%$.

heterogeneous LA wall injury was seen IPA in all patients with similar amounts of NE and HE tissue. Results showing HE lesions IPA were not surprising, as hyperenhancement on LGE in the early post-ablation period has been described by several investigators and appears to result from a spectrum of injuries from inflammation to necrosis (8,9,15,19). However, we did not expect to find large regions of NE tissue in equal proportion to HE tissue. These data expand our understanding of acute ablation injury and open new avenues for study of lesion formation. **NE lesions and no-reflow.** That acute ablation injury results in NE lesions in the LA myocardium is a novel finding in this study. NE lesions were present in all patients IPA and accounted for a nearly equal proportion of the acute injuries on LGE (NE 35.9% vs. HE 36.3%) using methods described here. Although published studies have focused on RF injuries and the resulting hyperenhancement, our data clearly show that ablation results in nonuniform injury with more complex tissue characteristics on LGE than previously described. On further investigation of these NE lesions, we found MRI characteristics consistent with no-reflow phenomena (Fig. 7).

Although NE tissue with no-reflow characteristics has not previously been described IPA in the left atrium, acute ablation injury to the canine ventricular myocardium with similar contrast voids on MRI was reported by Dickfeld *et al.* (20). In their study, acute RF injury to the epicardial surface of the ventricle in dogs resulted in 4 distinct phases seen on contrast MRI. The phases included an early and prolonged signal void followed by increasing tissue enhancement and eventual loss of enhancement. Histological examination of the RF lesions demonstrated findings consistent with an extreme form of the no-reflow phenomenon, with coagulation and contraction band necrosis and com-

plete loss of cellular and vascular architecture. A similar no-reflow phenomenon was described on first-pass contrast enhanced MRI in the setting of acute myocardial infarction (21). In acute ischemic injury, hypoenhancement in the endocardial core due to severe disruption in regional blood flow is thought to represent occlusion of microvasculature with blood cells and other debris that define no-reflow (22,23).

Acute lesions and resultant scar formation. Results from our 37-patient cohort show that RF ablation results in acute and extensive injury involving 72.0% of the LA wall, while only 33.9% of the wall is permanently scarred at 3 months. We also performed more detailed comparisons of injuries from IPA and 3moPA scans, which was complex because of registration challenges resulting from differences in LA wall size and shape at 2 time points. Unique application of 3D processing tools with deformable surface registration enabled matching locations IPA and 3moPA and comparisons between tissue types. This analysis was labor intensive and was therefore performed on only a subset of patients with the best-quality scans. From this 10-patient subset analysis, we showed that NE regions of no-reflow were nearly 2-fold more likely to predict permanent scar (59.0% vs. 30.6%, $p < 0.0001$). As NE tissue on LGE constituted a similar amount of the LA wall as HE tissue (34.3% vs. 37.7%, $p = \text{NS}$), these data indicate that a significantly greater amount of HE tissue represents transient injury, while NE tissue better reflects permanent injury.

Some tissue identified as normal on IPA imaging registered with scarring at 3-month follow-up (10.4%). This appears to reflect errors that result from the registration, lesion segmentation, and method of longitudinal compari-

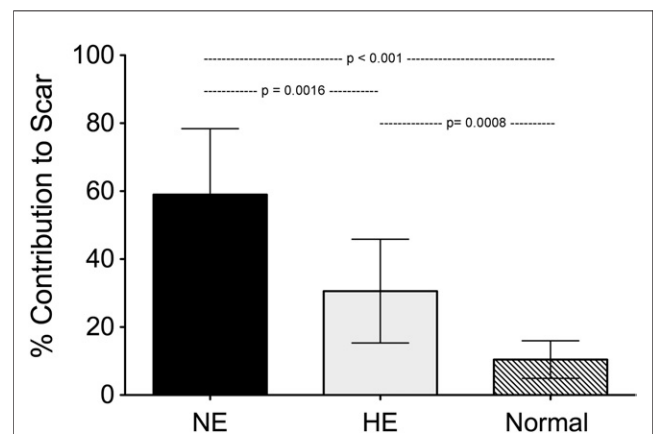


Figure 5 Percentage Left Atrial Wall Scar 3 Months Post-Ablation That Results From the Acute NE or HE Lesions Immediately Post-Ablation

Nonenhancing (NE) tissue ($59.0 \pm 19\%$) contributes nearly 2-fold more to permanent scar than hyperenhancing (HE) tissue ($30.6 \pm 15\%$). Some normal tissue ($10.4 \pm 5\%$) also resulted in scar, reflecting the limitations of the magnetic resonance imaging scan and registration methods. Paired *t*-test comparisons were all statistically significant: NE versus HE, $p = 0.0016$; NE versus normal, $p < 0.0001$; and HE versus normal, $p = 0.0008$.

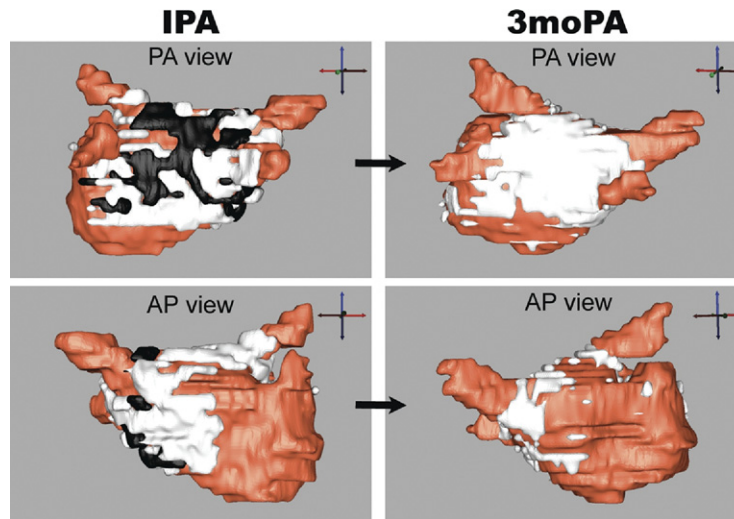


Figure 6 Late Gadolinium Enhancement No-Reflow Predicts Late Scarring

Using 3-dimensional nonrigid processing methods allows more direct comparisons of left atrial wall injury at 2 different time-points. Immediately post-ablation (IPA) shows 60% nonenhancing (**black**) regions of no-reflow converting to scar (**white**) 3 months post-ablation (3moPA). Only 30% of early hyperenhancing tissue persists at 3-month follow-up. Normal tissue is shown in **orange**. AP = anterior-posterior; PA = posterior-anterior.

son. Still, the purpose of this study was to report on the potential for using NE regions in the LA wall immediately after ablation to improve prediction of late scar. Our results shed valuable light on the nature of NE tissue and open a new avenue for the evaluation of IPA injury. Although the registration of the 2 scans is important for this and perhaps future study of lesion formation and late scarring, in clinical practice, scan registration may not be critical because the

goal would be to use IPA MRI data to guide therapy at the time of ablation.

Acute HE tissue is a poor predictor of late scar. LGE performed IPA showed HE in greater than one-third of the LA wall. However, 3moPA, only 30.6% of the immediate HE tissue resulted in permanent scar. These data indicate that in the IPA period, HE tissue reflects transient inflammation and edema to a greater extent than tissue necrosis leading to permanent scar. These findings are not surprising, given the known kinetics of gadolinium. Gadolinium contrast is an extravascular agent that demonstrates delayed washout in tissue with increased extravascular space. As a result, enhancement is seen not only in necrotic or scarred tissue but also in regions of inflammation. For this reason, HE tissue on LGE in the early hours to days after ablation helps identify ablated tissue but does not necessarily reflect permanent injury. Data presented here are consistent with our prior published work showing LA wall enhancement on LGE MRI 24 h after ablation that overestimates scarring at 3 months (15).

LA wall scar and procedural outcome. The extent of LA wall scar assessed quantitatively by LGE MRI 3moPA predicts procedural success after AF ablation. Our data demonstrate no recurrences during 1-year follow-up when a moderate amount of scarring (>23% of LA wall volume) results from ablation injury. These findings are consistent with those of other studies showing improved procedure success with a greater degree of LA scar or more complete tissue injury after pulmonary vein isolation (12,14,24). In our previously published work in 2008 (12), we reported that arrhythmia recur-

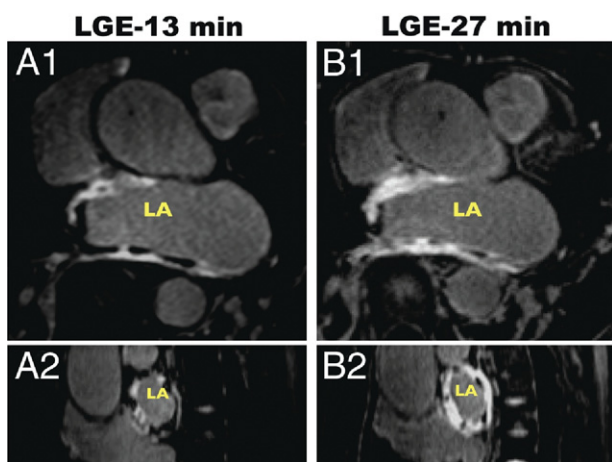


Figure 7 Serial LGE Images Demonstrate No-Reflow

Dark nonenhancing regions in the left atrial wall immediately post-ablation on late gadolinium enhancement (LGE) acquired 13 min after gadolinium contrast injection begin to hyperenhance on repeat imaging at 27 min. Axial (**A1, B1**) and sagittal (**A2, B2**) views are shown. LA = left atrium.

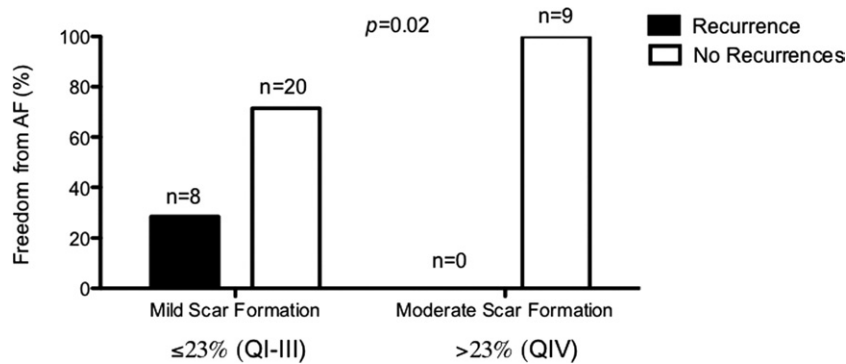


Figure 8 AF Ablation Procedural Success and Association With LA Wall Scar

High procedure success was seen in patients with >23% of left atrial (LA) wall volume scarring on late gadolinium enhancement magnetic resonance imaging, while recurrences were significantly higher in the lower quartile (Q) groups with injury <23%. Procedure success was defined as freedom from atrial fibrillation (AF) during 1-year post-ablation follow-up period. Overall procedure success was 78.4% at 1 year.

rence correlated with the degree of LA wall enhancement, with >13% scar best predicting freedom from AF. Although the present data show better prediction of success with a greater percentage of wall scar, direct comparisons are difficult to make because the present study was performed using different pulse sequence parameters on a higher field magnet (3- vs. 1.5-T) resulting in improved image quality and scar quantification. Nevertheless, the data are consistent in both studies as procedure success is predicted by degree of LA wall scar.

Factors affecting tissue contrast on LGE MRI. The tissue kinetics of gadolinium contrast and physiologic mechanisms of myocardial enhancement on contrast-enhanced MRI have been well studied in acute myocardial infarction and reperfusion injury models (22,23,25,26). Areas of hypoenhancement are believed to be due to delayed contrast penetration and hyperenhancement due to slow contrast washout. Ultimately, the specific LGE imaging characteristics will depend to a large extent on the injury produced, regional differences in tissue wash-in and wash-out kinetics, and the timing of image acquisition after contrast injection. To reduce the impact of variable tissue contrast that may be introduced by different timing of LGE imaging, we selected for scans performed within a relatively tight window timed 15 ± 3 min after contrast injection.

Study limitations. MRI characteristics of no-reflow on LGE MRI will benefit from detailed histological studies, which were not possible in this human study. The NE regions on LGE may represent the no-reflow phenomenon alone or a combination of other injuries, such as local thrombus formation. Also, the sample size was small ($n = 10$) for the detailed quantitative analysis of the LGE injuries seen IPA and 3moPA using 3D nonrigid deformation processing methods. A larger patient population will help further define the contributions of HE and NE injury to permanent scar.

Conclusions

LGE MRI has been used weeks to months after AF ablation to determine the extent of scarring, which is associated with patient outcome. In addition, in patients requiring a second procedure for recurrent AF, LGE MRI can help identify gaps in ablation lines that can result in procedure failure. The significant association we demonstrate between no-reflow and permanent scarring may expand the utility of LGE MRI to help guide ablation at the time of the procedure. With the growing interest in electrophysiology-MRI suites and the goal to achieve real-time MRI-guided ablation, continued study of early lesion imaging will be important.

Acknowledgments

The authors are grateful for the dedication and hard work of the cardiac MRI technologists in the Radiology Department at the University of Utah, including Josh Bertola, RT, Karl Bohman RT, and Stacey Calderon, RT.

Reprint requests and correspondence: Dr. Christopher McGann, Cardiology Division, University of Utah Health Sciences Center, 30 North 1900 East, Salt Lake City, Utah 84132. E-mail: chris.mcgann@hsc.utah.edu.

REFERENCES

1. Fuster V, Rydén L, Cannom DS, et al. ACC/AHA/ESC 2006 guidelines for the management of patients with atrial fibrillation—executive summary: a report of the American College of Cardiology/American Heart Association Task Force on Practice Guidelines and the European Society of Cardiology Committee for Practice Guidelines (Writing Committee to Revise the 2001 Guidelines for the Management of Patients with Atrial Fibrillation). *J Am Coll Cardiol* 2006;48:e149–246.
2. Go AS, Hylek EM, Phillips KA, et al. Prevalence of diagnosed atrial fibrillation in adults: national implications for rhythm management and stroke prevention: the Anticoagulation and Risk Factors in Atrial Fibrillation (ATRIA) study. *JAMA* 2001;285:2370–5.

3. Pappone C, Rosanio S, Oreto G, et al. Circumferential radiofrequency ablation of pulmonary vein ostia: a new anatomic approach for curing atrial fibrillation. *Circulation* 2000;102:2619-28.
4. Oral H, Scharf C, Chugh A, et al. Catheter ablation for paroxysmal atrial fibrillation: segmental pulmonary vein ostial ablation versus left atrial ablation. *Circulation* 2003;108:2355-60.
5. Mansour M, Ruskin J, Keane D. Efficacy and safety of segmental ostial versus circumferential extra-ostial pulmonary vein isolation for atrial fibrillation. *J Cardiovasc Electrophysiol* 2004;15:532-7.
6. Oral H, Pappone C, Chugh A, et al. Circumferential pulmonary-vein ablation for chronic atrial fibrillation. *N Engl J Med* 2006;354:934-41.
7. Lardo AC, McVeigh ER, Jummussirikul P, et al. Visualization and temporal/spatial characterization of cardiac radiofrequency ablation lesions using magnetic resonance imaging. *Circulation* 2000;102:698-705.
8. Knowles B, Caulfield D, Cooklin M, et al. Three-dimensional visualization of acute radiofrequency ablation lesions using MRI for the simultaneous determination of the patterns of necrosis and edema. *IEEE Trans Biomed Eng* 2011. In press.
9. McGann CJ, Blauer J, Vijayakumar S, et al. Acute injury immediately post atrial fibrillation ablation defined by MRI (abstr). *J Cardiovasc Magn Reson* 2010; 12 Suppl:M1.
10. Peters DC, Hsing K, Kisinger KV, et al. T2-weighted imaging of the left atrium acutely after pulmonary vein isolation demonstrates wall thickening and edema (abstr). Paper presented at: 17th Scientific Meeting & Exhibition of the International Society for Magnetic Resonance in Medicine; Honolulu, HI; April 18-24, 2009.
11. Peters DC, Wylie JV, Hauser TH, et al. Detection of pulmonary vein and left atrial scar after catheter ablation with three-dimensional navigator-gated delayed enhancement MR imaging: initial experience. *Radiology* 2007;243:690-5.
12. McGann CJ, Kholmovski EG, Oakes RS, et al. New magnetic resonance imaging-based method for defining the extent of left atrial wall injury after the ablation of atrial fibrillation. *J Am Coll Cardiol* 2008;52:1263-71.
13. Segerson NM, Daccarett M, Badger TJ, et al. Magnetic resonance imaging-confirmed ablative debulking of the left atrial posterior wall and septum for treatment of persistent atrial fibrillation: rationale and initial experience. *J Cardiovasc Electrophysiol* 2010;21:126-32.
14. Peters DC, Wylie JV, Hauser TH, et al. Recurrence of atrial fibrillation correlates with the extent of post-procedural late gadolinium enhancement: a pilot study. *J Am Coll Cardiol Img* 2009;2:308-16.
15. Badger TJ, Oakes RS, Daccarett M, et al. Temporal left atrial lesion formation after ablation of atrial fibrillation. *Heart Rhythm* 2009;6: 161-8.
16. Glaunes J, Trouve A, Younes L. Diffeomorphic matching of distributions: a new approach for unlabeled point-sets and sub-manifolds matching. Paper presented at: IEEE Computer Society Conference on Computer Vision and Pattern Recognition; Washington, DC; June 27 to July 2, 2004.
17. Vaillant M, Glaunes J. Surface matching via currents. *Inf Process Med Imaging* 2005;19:381-92.
18. Ha L, Prastawa M, Gerig G, Gilmore J, Silva C, Joshi S. Image registration driven by combined probabilistic and geometric descriptors. *Med Image Comput Comput Assist Interv* 2010;13:602-9.
19. Yokokawa M, Tada H, Koyama K, et al. Thickening of the left atrial wall shortly after radiofrequency ablation predicts early recurrence of atrial fibrillation. *Circ J* 2010;74:1538-46.
20. Dickfeld T, Kato R, Zviman M, et al. Characterization of radiofrequency ablation lesions with gadolinium-enhanced cardiovascular magnetic resonance imaging. *J Am Coll Cardiol* 2006;47:370-8.
21. Rogers WJ Jr, Kramer CM, Geskin G, et al. Early contrast-enhanced MRI predicts late functional recovery after reperfused myocardial infarction. *Circulation* 1999;99:744-50.
22. Lima JA, Judd RM, Bazille A, Schulman SP, Atalar E, Zerhouni EA. Regional heterogeneity of human myocardial infarcts demonstrated by contrast-enhanced MRI. Potential mechanisms. *Circulation* 1995;92: 1117-25.
23. Judd RM, Lugo-Olivieri CH, Arai M, Kondo T, et al. Physiological basis of myocardial contrast enhancement in fast magnetic resonance images of 2-day-old reperfused canine infarcts. *Circulation* 1995;92: 1902-10.
24. Verma A, Kilicaslan F, Pisano E, et al. Response of atrial fibrillation to pulmonary vein antrum isolation is directly related to resumption and delay of pulmonary vein conduction. *Circulation* 2005;112:627-35.
25. Kim RJ, Fieno DS, Parrish TB, et al. Relationship of MRI delayed contrast enhancement to irreversible injury, infarct age, and contractile function. *Circulation* 1999;100:1992-2002.
26. Wu KC, Zerhouni EA, Judd RM, et al. Prognostic significance of microvascular obstruction by magnetic resonance imaging in patients with acute myocardial infarction. *Circulation* 1998;97:765-72.

Key Words: ablation ■ atrium ■ fibrosis ■ magnetic resonance imaging.